揮発性有機ハロゲン化合物を可視化する有機色素含有ポリウレタン材料の開発

【概要】揮発性有機ハロゲン化合物を可視する有機色素含有ポリウレタン材料の開発を目指して、カウンターアニオンを有する新規な D-A 型および D-π-A 型ピリジニウム色素を分子設計・合成した。開発したこれらの色素が子内電荷移動特性に基づく光吸収帯を有し、さらにその光吸収極大波長が有機ハロゲン溶媒中においてのみ特異的に長波長シフトするオルガノハロゲノクロミズム(Organohalogenochromism: OHC)を発現することがわかった。以下に、D-A型および D-π-A型ピリジニウム色素の OHC について追究した結果について報告する。

## Introduction

In halogenated solvents, including dichloromethane and dibromomethane, some organic dyes exhibit a significant hypsochromic or bathochromic shift of photoabsorption band that has long been noticed by many researchers. Nevertheless, such specific solvatochromism has only recently been termed organohalogenochromism (OHC), and thus it is recognized as a photophysical phenomenon that is totally different from a common solvatochromism depending on solvent polarity parameter  $(E_T(30))$ , normalized solvent polarity value  $(E_T^N)$  or dielectric constant ( $\varepsilon_r$ ) of solvent. So far bathochromic shift-type OHC (b-OHC) has been found in a certain donor-π-acceptor (D- $\pi$ -A) type cationic dyes bearing a counter anion which are composed of a strong electron-donating (D) moiety dialkyl or diaryl amino group) and a strong electronwithdrawing (A) cationic moiety (e.g. pyridinium or benzothiazolium ring) linked by a  $\pi$ -conjugated bridge, so that they exhibit an intense photoabsorption band based on the intramolecular charge transfer (ICT) from the D to the A moiety. However, the research on OHC remains in a phenomenological investigation, organohalogenochromic dyes have a great potential for developing optical sensing system for visualization and detection of toxic Therefore, in order to provide a direction in the molecular design for expressing OHC reliably and to create functional dye materials for colorimetric detection of VOHCs, further fundamental studies to lead to comprehensive elucidation of the origin of OHC are absolutely required.

Thus, in this work, in order to gain a deeper insight into the origin of organohalogenochromism (OHC) with the objective of XB between the organohalogen and the dye molecules, we have designed and prepared the D- $\pi$ -A type and D-A type pyridinium dyes **OD2** and **KK2** bearing bromide ion (Br<sup>-</sup>) as a counter anion which has julolidine part as the D moiety (Figure 1). It is expected that the difference in the electronic structure between **OD2** and **KK2** affects the magnitude of OHC characteristics. Herein, based on the <sup>1</sup>H NMR spectroscopies, cyclic voltammetry (CV), the single-crystal X-ray structural analyses, and the theoretical investigations using density functional theory (DFT) calculation, we offer the mechanism for expression of OHC by the influence of XB on the electronic structure of dye molecule.

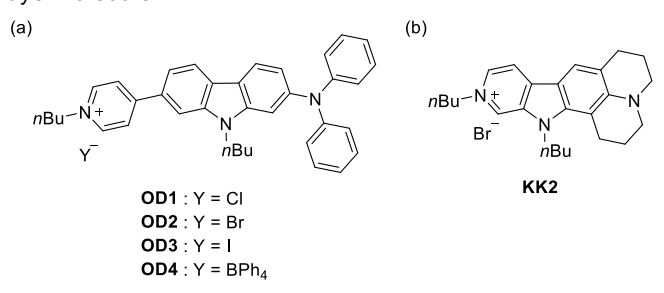
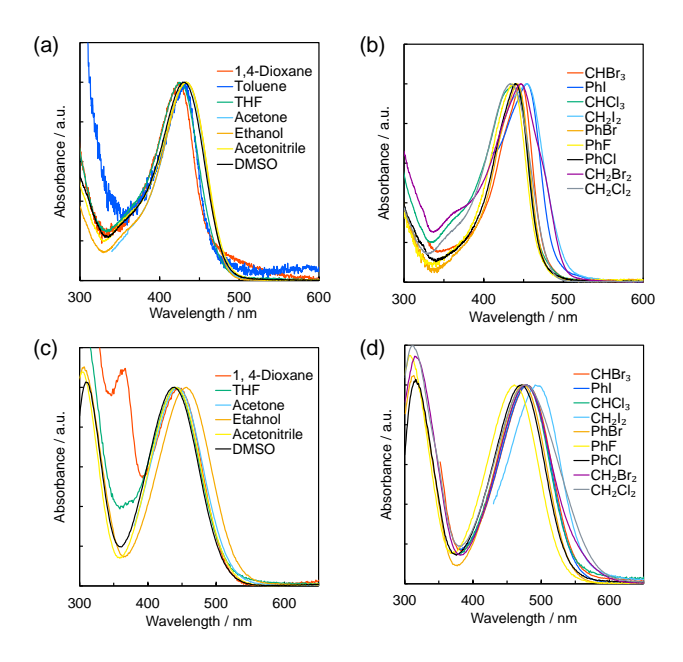


Figure 1. Chemical structures of (a) D- $\pi$ -A type pyridinium dyes OD1-4 in previous work and (b) D-A type pyridinium dye KK2 in this work.

## **Results and Discussion**

The D-A type pyridinium dye **KK2** was prepared from the D-A type pyridine dye **ET-1** and *n*-butyl bromide. **KK2** shows the photoabsorption maximum wavelength ( $\lambda_{max}^{abs}$ ) at around 420–455 nm originating form ICT excitation from julolidine part as D moiety to a pyridinium ring as A moiety both in halogenated and non-halogenated solvents (Figure 2), and thus the ICT-based  $\lambda_{max}^{abs}$  of **KK2** appear in a shorter wavelength region compared to those (ca. 440–495 nm) of **OD2**. Meanwhile, the molar extinction coefficient values ( $\varepsilon_{max} = ca. 8500–23500 \, M^{-1} \, cm^{-1}$ ) of  $\lambda_{max}^{abs}$  for **KK2** 

are smaller than those ( $\varepsilon_{\text{max}}$  = ca. 16 000–40 500 M<sup>-1</sup> cm<sup>-1</sup>) for **OD2**.



**Figure 2.** Photoabsorption spectra of (a) **KK2** and (c) **OD2** in non-halogenated solvents and (b) **KK2** and (d) **OD2** in halogenated solvents.

In order to make clear the influence of solvent polarity on the ICT-based  $\lambda_{\text{max}}^{\text{abs}}$  of **KK2** and **OD2**, the wavenumbers  $(v_{max}^{abs})$  of the  $\lambda_{max}^{abs}$  were plotted against solvent polarity parameter  $(E_T(30))$ , polarizability density  $(n^2-1/2n^2+1)$ ;  $f(n^2)$ ), orientation polarizability ( $\Delta f$ ), and dielectric constant  $(\varepsilon_r)$  of solvent (Figure 3a-h). For both the dyes, these plots do not follow a linear relationship between them and remain on almost plateau among non-halogenated solvents, indicating that the  $v_{max}^{abs}$  are nearly independent of solvent polarity. On the other hand, obviously, one can see that KK2 and OD2 show a significant bathochromic shift of  $\lambda_{\max}^{abs}$ , that is, shifting of  $\nu_{\max}^{abs}$  to lower wavenumber, in halogenated solvents compared with the  $\lambda_{max}^{abs}$  ( $v_{max}^{abs}$ ) in non-halogenated solvents; while the  $\varepsilon_r$  value (7.52) of THF is quite similar to that (7.77) of dibromomethane, the  $\lambda_{\max}^{abs}$ (446 nm and 475 nm) of KK2 and OD2 in dibromomethane appear at a longer wavelength region by 21 nm and 35 nm, respectively, than those (425 nm and 440 nm) in THF. It is worth mentioning here that in halogenated solvents the ICTbased  $\lambda_{\text{max}}^{\text{abs}}$  (ca. 435-455 nm) of **KK2** occur at a shorter wavelength region (a higher wavenumber range) compared to those (ca. 460-495 nm) of OD2. In the course of exploring the influences of halogenated solvents on the ICT-based  $\lambda_{max}^{abs}$  ( $V_{max}^{abs}$ ), we found that there is a good relationship between the most positive surface electrostatic potential ( $V_{S,max}$ ) values associated with the most positive σ-hole on halogen atoms in organohalogen molecule and the  $v_{\text{max}}^{\text{abs}}$ , indicating influence of the formation of halogen

bond (XB) on the electronic structure of dye molecule. In general, the strength of XB regarding halogen atom (X) increases with an increase in the size of the halogen atom as Lewis acid, that is, in the order of F < Cl < Br < I. Indeed, the plots of the  $v_{\max}^{abs}$  against the  $V_{S,\max}$  values demonstrated that for both KK2 and OD2 the  $v_{\rm max}^{\rm abs}$ decrease linearly with the increase in the  $V_{S,max}$  values (Figure 3i, j). Consequently, the fact revealed that the b-OHC of the D-A and D- $\pi$ -A pyridinium dyes may be associated with the formation of XB between the halogen atom of organohalogen molecule and the counter anion of the dye molecule (Figure 3i, j). However, the correlation coefficient ( $R^2$ ) value (0.235) and the slope ( $m_s$ ) value (-22.2) of the calibration curve for KK2 are lower than those (0.733 and -45.1, respectively) for OD2, indicating that the b-OHC characteristic of KK2 is lower than that of OD2.

Thus, in order to investigate the solvent effect on the electronic structure of the D-A and D- $\pi$ -A pyridinium dyes, we performed the <sup>1</sup>H NMR spectral measurements of KK2 and **OD2** in acetonitrile- $d_3$  and THF- $d_8$  as non-halogenated solvent and dichloromethane- $d_2$  as a halogenated solvent (Figure 4). One can see that there is a slight difference in the chemical shifts of the protons for D or D- $\pi$  moiety, that is, the julolidine moiety for KK2 or the diphenylamino group and its nearby carbazole part for OD2, between the three deuterated solvents. On the other hand, significant differences in the chemical shifts of A moiety were observed between halogenated and non-halogenated solvents. For KK2 the signals of  $H_a$  and  $H_b$  of pyridinium ring in dichloromethane- $d_2$  show upfield shifts compared to those in acetonitrile- $d_3$  and THF- $d_8$ , while the signal for  $H_c$  of the pyridinium ring in dichloromethane- $d_2$  show upfield and downfield shift, respectively, compared to those in THF-d<sub>8</sub> and acetonitrile-d<sub>3</sub>. Meanwhile, for **OD2** the signals of H<sub>b</sub> of pyridinium ring, H<sub>c</sub> and H<sub>d</sub> of carbazole part near the pyridinium ring in dichloromethane- $d_2$  show upfield shifts compared to those in acetonitrile- $d_3$  and THF- $d_8$ , while the signal for H<sub>a</sub> of the pyridinium ring in dichloromethane-d<sub>2</sub> show upfield and downfield shift, respectively, compared to those in THF- $d_8$  and acetonitrile- $d_3$ , as with the case of **KK2**. This result suggests a decrease in the ring current of the pyridinium and its nearby aromatic rings in halogenated compared non-halogenated solvents. solvents, to Consequently, the fact offers the occurrence of intermolecular interaction between the organohalogen and the dye molecules, that is, the formation of XB between the halogen atom of organohalogen molecule and the counter anion of the dye molecule, leading to a decrease in the ring current of the pyridinium and its nearby aromatic rings in halogenated solvents.

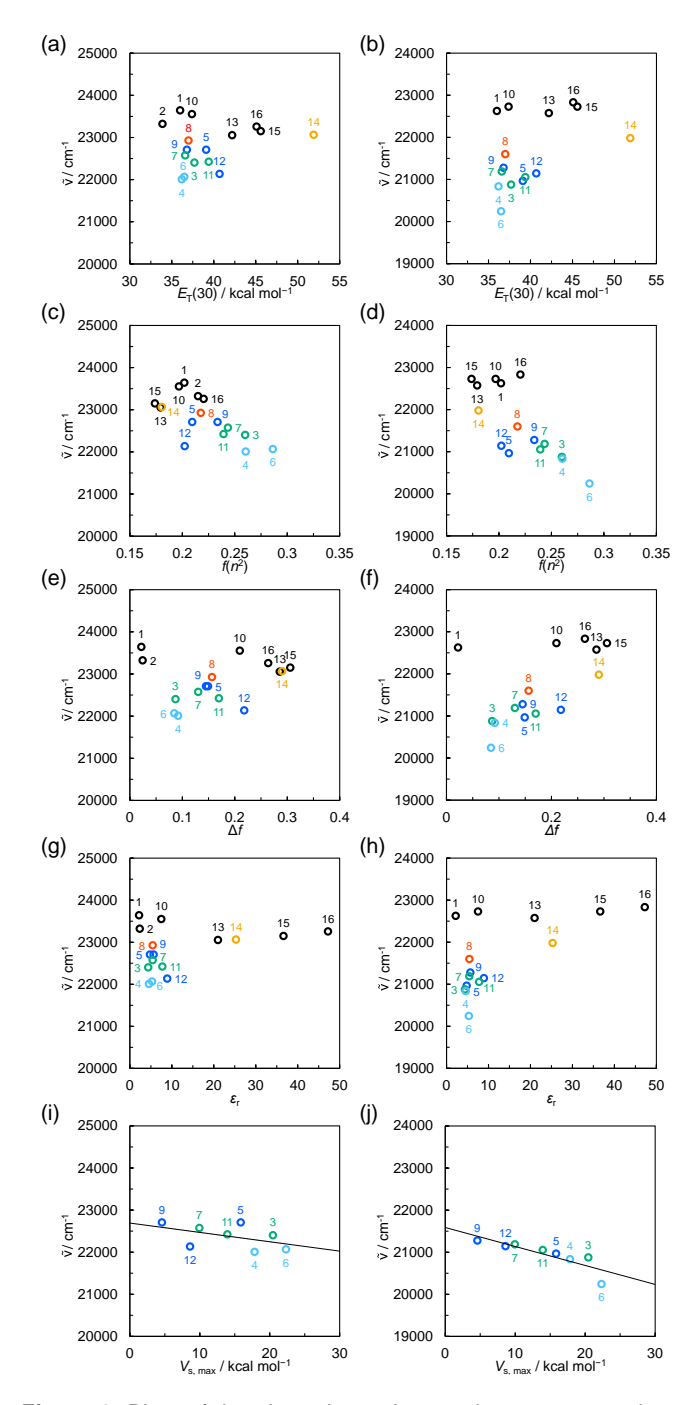
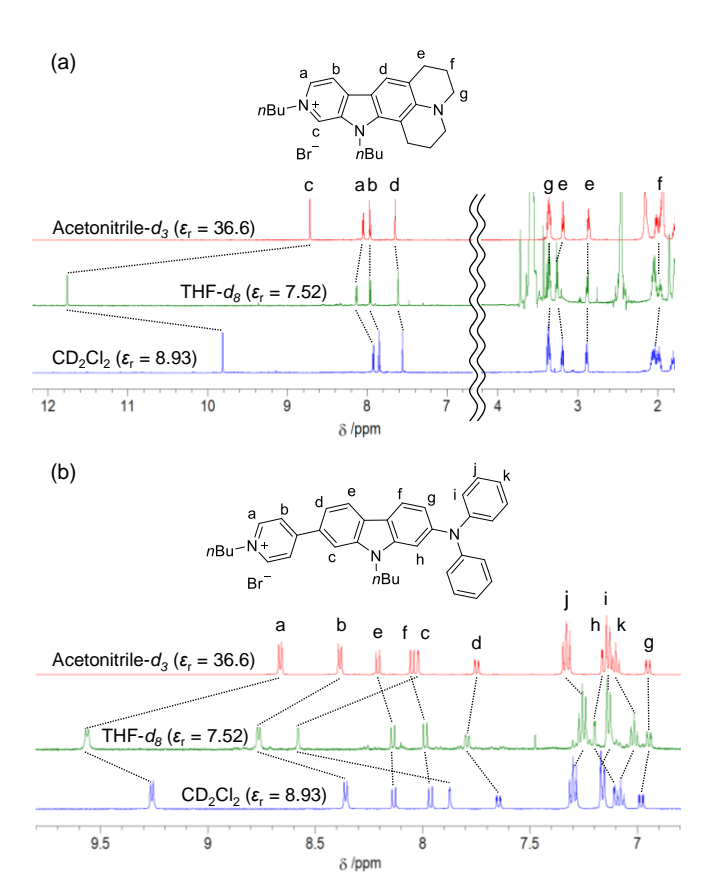


Figure 3. Plots of the photoabsorption maximum wavenumber ( $\nu$ ) of **KK2** against (a) solvent polarity parameter ( $E_T(30)$ ), (c) polarizability density  $(n^2-1/2n^2+1; f(n^2))$ , (e) orientation polarizability ( $\Delta f$ ), (g) dielectric constant ( $\varepsilon_r$ ) of solvent, and (h) the most positive surface electrostatic potential  $(V_{S,max})$ associated with the most positive  $\sigma$ -hole on halogen atoms in organohalogen solvent. Plots of the photoabsorption maximum wavenumber (V) of **OD2** against (b)  $E_T(30)$ , (d)  $f(n^2)$ , (f)  $\Delta f$ , (h)  $\varepsilon_{\rm r}$  of solvent, and (j)  $V_{\rm S,max}$ . The numbers refer to 1: 1,4-dioxane, 2: toluene, 3: CHBr<sub>3</sub>, 4: PhI, 5: CHCl<sub>3</sub>, 6: CH<sub>2</sub>l<sub>2</sub>, 7: PhBr, 8: PhF, 9: PhCI, 10: THF, 11: CH<sub>2</sub>Br<sub>2</sub>, 12: CH<sub>2</sub>CI<sub>2</sub>, 13: Acetone, 14: Ethanol, 15: acetonitrile, and 16: DMSO. The circles in black, red, blue, green, purple, light blue, and orange show nonhalogenated solvents, fluorobenzene, chlorinated solvents, brominated solvents, iodinated solvents, and respectively.



**Figure 4.** <sup>1</sup>H NMR spectra of (a) **KK2** and (b) **OD2** in acetonitrile- $d_3$  and THF- $d_8$ , and dichloromethane- $d_2$  (CD<sub>2</sub>Cl<sub>2</sub>).

Furthermore, in order to reveal the influence of the HOMO and LUMO energy levels of the D-A and D- $\pi$ -A pyridinium dyes on the b-OHC, we performed cyclic voltammetry (CV) in acetonitrile or dichloromethane 0.1 Μ tetrabutylammonium (Bu<sub>4</sub>NCIO<sub>4</sub>) to determine exactly the redox potential. The potentials were internally referenced ferrocene/ferrocenium (Fc/Fc+). The cyclic voltammograms showed an irreversible oxidation wave at ca. 0.40-0.50 V for KK2 and ca. 0.45-0.55 V for OD2, and in acetonitrile the oxidation peak potential  $(E_{pa}^{ox})$  for **KK2** is cathodically shifted by ca. 0.1 V, compared to that for OD2. Moreover, it was found that the  $E_{pa}^{ox}$  for KK2 and OD2 in dichloromethane are a slightly anodic and cathodic shift by 0.05 V and 0.06 V, respectively, compared to those in acetonitrile. Meanwhile, any obvious reduction wave did not appear within the potential window (-1.5 V-0 V versus Fc/Fc<sup>+</sup>). Thus, the HOMO energy levels ( $-[E_{pa}^{ox} + 4.8] \text{ eV}$ ) versus vacuum level were estimated from the  $E_{pa}^{ox}$ , and the corresponding LUMO energy levels were estimated from the  $E_{pa}^{ox}$  and the onsets (optical energy gap:  $E_{q}^{opt}$ ) of the photoabsorption spectra in the acetonitrile dichloromethane solution (Figure 5). Both in acetonitrile and dichloromethane, the HOMO and LUMO energy levels (ca. -5.25 eV and ca. -2.80 eV, respectively) of KK2 are higher than those (ca. -5.30 eV and ca. -3.15 eV,

respectively) of OD2. It is worth noting here that the LUMO energy levels (-2.84 eV and -3.26 eV, respectively) of KK2 and OD2 in dichloromethane are much lower than those (-2.74 eV and -3.07 eV, respectively) in acetonitrile, although the HOMO energy levels (-5.27 eV and -5.26 eV, respectively) of KK2 and OD2 in dichloromethane are similar to those (-5.22 eV and -5.32 eV, respectively) in acetonitrile. Consequently, for both KK2 and OD2 the bathochromic shift of  $\lambda_{max}^{abs}$  in halogenated solvents relative to those in non-halogenated solvents is attributed to the stabilization of the LUMO energy level, leading to a decrease in the HOMO-LUMO band gap. In addition, it was revealed that the lowering in the LUMO energy level of OD2 with change in solvent from acetonitrile to dichloromethane is larger than that in KK2, resulting in the pronounced b-OHC of OD2.

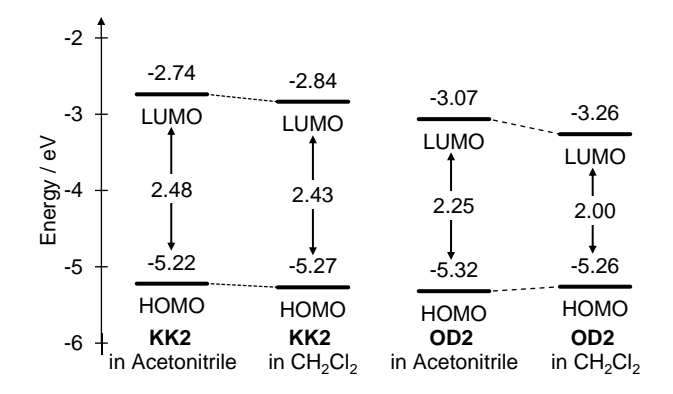


**Figure 5.** Energy level diagram for HOMO and LUMO of **KK2** and **OD2** estimated from cyclic voltammetry and photoabsorption spectral measurement.

single-crystal X-ray structural successfully made for KK2 as well as OD2 (Figure 6). There are two crystallographically independent dye molecules in the crystal structure of OD2. The bromide ion is located near pyridinium rings and its nearby carbazole part in a pair of dye molecules: the distances between Br<sup>-</sup>(1) and C(53) [or Br<sup>-</sup>(2) and C(16)\*] in pyridinium ring and between Br<sup>-</sup>(1) and C(52) [or Br-(2) and C(15)\*] in pyridinium ring are ca. 3.58 Å and 3.64 Å, respectively, and the distances between Br<sup>-</sup>(1) and C(11) in carbazole moiety and between Br<sup>-</sup>(2) and C(48) in carbazole moiety are ca. 3.80 Å and 3.79 Å, respectively. Similarly, for KK2 the bromide ion is located near pyridinium rings in two adjacent dye molecules: the distances between Br-(1) and C(5) in pyridinium ring and between Br-(1) and C(9) in pyridinium ring are ca. 3.49 Å and 3.54 Å, respectively.

Thus, in order to reveal the molecular orbitals of **KK2** and **OD2** in THF or dichloromethane, we performed the DFT calculations by the self-consistent reaction field (SCRF) method using the integral equation formalism polarizable

continuum model (IEFPCM) based on B3LYP/6-31G+(d,p) level after geometrical optimizations at M062X/6-31G+(d,p) level using the molecular structures derived from the singlecrystal X-ray structural analysis. The DFT calculations demonstrated that for KK2 in both THF dichloromethane the HOMO and LUMO are delocalized over the whole molecule. In contrast, for OD2 the HOMO is localized on the (diphenylamino)carbazole moiety and the LUMO is mostly localized on pyridinium rings and its nearby carbazole part, indicating that the HOMO and LUMO distributions for the molecular structure are adequately separated (Figure 7). Accordingly, the photoexcitation of OD2 induces intense ICT characteristics from the (diphenylamino)carbazole unit as a  $D-\pi$  moiety to the pyridinium ring as A moiety, compared to that of KK2. Furthermore, the DFT calculations at B3LYP/6-31G(d,p) for the molecular structures with the XB (CIH<sub>2</sub>C-CI···Br<sup>-</sup>) or the complex such as [CIH<sub>2</sub>C-CI·Br]<sup>-</sup> between dichloromethane and bromide ion which has been geometrically optimized at M062X/6-31G(d,p) level, showed that the HOMO and LUMO distributions of KK2 and OD2 with the XB are similar to those without the XB. Indeed, for both KK2 and OD2, one can see little change in the HOMO and LUMO energy levels between the dye molecule with and without the XB that is not consistent with the experimental results from the CV and the photoabsorption spectral analyses (Figure 5). Thus, unfortunately, the DFT calculations in the current stage did not give a useful insight into the influence of XB on the expression of b-OHC for D-A and D- $\pi$ -A pyridinium dyes. Nevertheless, based on the experimental and theoretical results, it was suggested that the formation of XB or complex such as [R-X·Y] between the halogen atom of organohalogen molecule and the counter anion of the D-A or  $D-\pi-A$  pyridinium molecule induces the decrease in the ring current of pyridinium ring that the LUMO is mainly localized, resulting in expression of b-OHC due to the stabilization of the LUMO energy level. Moreover, it was revealed that the pronounced b-OHC of **OD2** relative to that of KK2 is attributed to the well-separated HOMO and LUMO distributions for OD2, leading to the intense ICT-based photoabsorption and a great perturbation to the LUMO energy level by the formation of XB or [R-X·Y]-. Consequently, this work offers a deeper insight into the mechanism for the expression and the origin of OHC. Meanwhile, in order to fully clarify the b-OHC with the objective of the XB, we would like to verify the formation of XB from the single-crystal X-ray structural analyses for the organohalogen molecules-inclusion dye crystals and then to perform the DFT calculation using the obtained molecular structure with the XB in the next work.

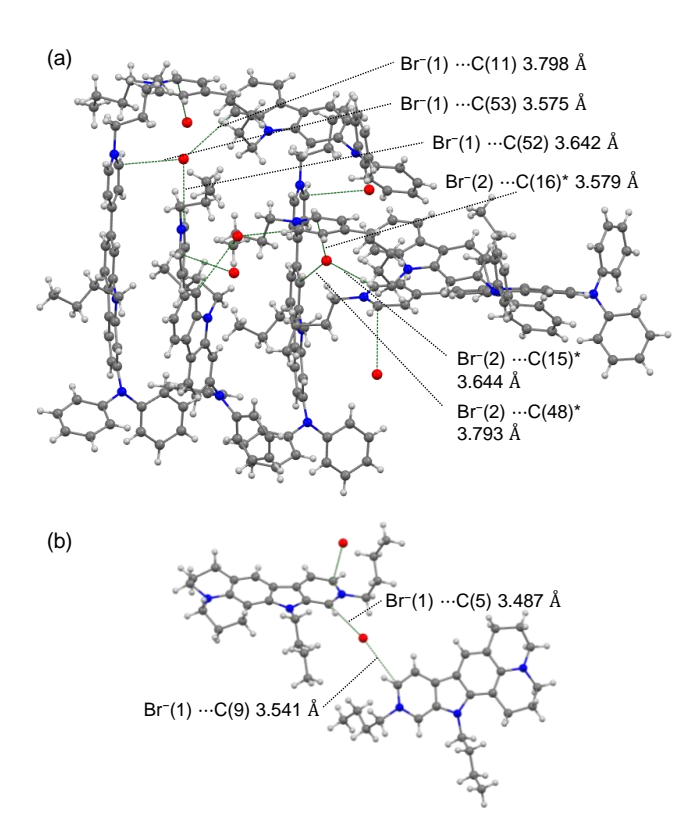


Figure 6. Crystal structures of (a) OD2 and (b) KK2.

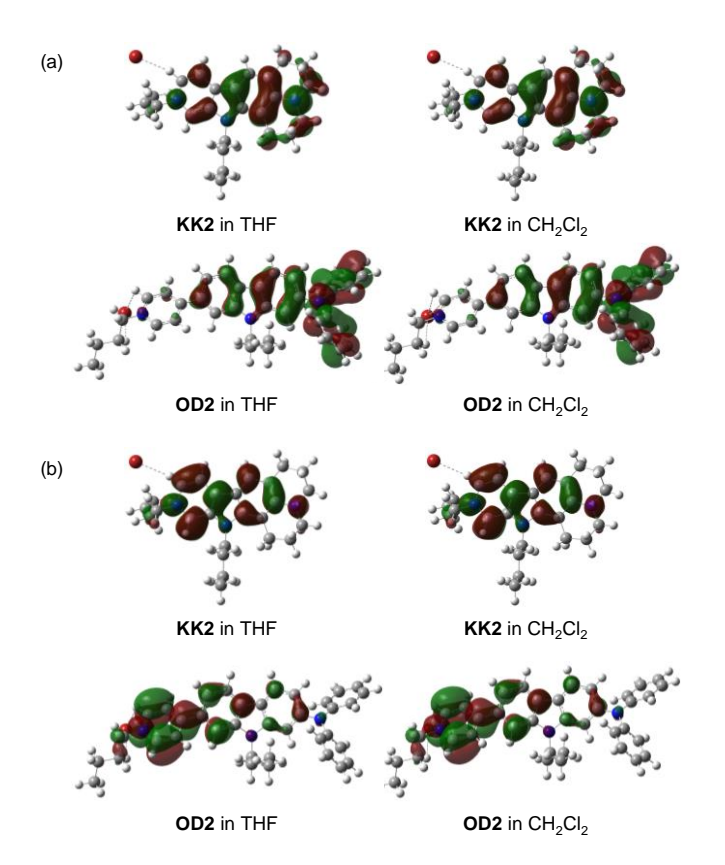


Figure 7. (a) HOMO and (b) LUMO of KK2 and OD2 derived from the DFT calculations by the self-consistent reaction field (SCRF) method using the integral equation formalism polarizable continuum Model (IEFPCM) based on B3LYP/6-31G+(d,p) level after geometrical optimizations at the M062X/6-31G+(d,p) level using the molecular structures of the single-crystal X-ray structural analysis.

## Conclusion

In this work, we attempted to elucidate the bathochromic shift-type OHC (b-OHC) of D-A and D- $\pi$ -A pyridinium dyes bearing halide ion as a counter anion with the objective of the intermolecular interaction between the organohalogen and the dye molecules. It was revealed that there is a good relationship between the most positive surface electrostatic potential ( $V_{S,max}$ ) values associated with the most positive  $\sigma$ -hole on halogen atoms in organohalogen molecule and intramolecular charge transfer (ICT)-based photoabsorption maximum wavenumbers (V~maxabs), indicating that the formation of halogen bond (XB) or complex such as [R-X·Y] between the halogen atom (X) of organohalogen molecule and the counter anion (Y-) of dye molecule contributes to the expression of b-OHC. The experimental and theoretical results revealed that the formation of XB or complex [R-X·Y]<sup>-</sup> induces the decrease in the ring current of pyridinium ring that the LUMO is mainly localized, resulting in expression of b-OHC due to the stabilization of the LUMO energy level. Moreover, the pronounced b-OHC of D- $\pi$ -A pyridinium dye relative to that of D-A pyridinium dye is attributed to the well-separated HOMO and LUMO distributions for the D- $\pi$ -A pyridinium dye, leading to the intense ICT-based photoabsorption and a great perturbation to the LUMO energy level by the formation of XB or [R-X·Y]-. Consequently, we believe that this work contributing to a deeper insight into the mechanism for the expression and the origin of OHC leads to development of organic dye possessing hypsochromic shift-type OHC (h-OHC) as well as modulation of b-OHC by selecting kinds of counter anions.

【今後の展望】本研究では、カウンターアニオンを有する新規な D-A 型および D-π-A 型ピリジニウム色素の OHC を明らかにすることができた。今後の取り組みとして、D-A 型および D-π-A 型ピリジニウム色素をポリウレタン樹脂塗料に分散させて基板に散布したポリウレタンコーティング膜および直接ポリマー化によるポリウレタンフィルムを作製し、揮発性有機ハロゲン化合物を接触させた際の色調変化を目視(画像取得)およびポータブル分光光度計を用いたその場測定による光吸収スペクトル測定を実施したい。

## 【発表論文】

- K. Kozuka, K. Imato and Y. Ooyama, *Chem. Asian J.*, 2025, doi.org/10.1002/asia.202500746. (Invited Article).
- K. Kozuka, K. Imato and Y. Ooyama, ChemPhotoChem, 2025, 9, e202400187 (Invited Concept Article).